CRREL

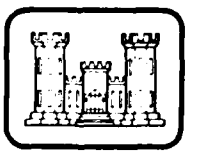

High-explosive cratering in frozen and unfrozen soils in Alaska

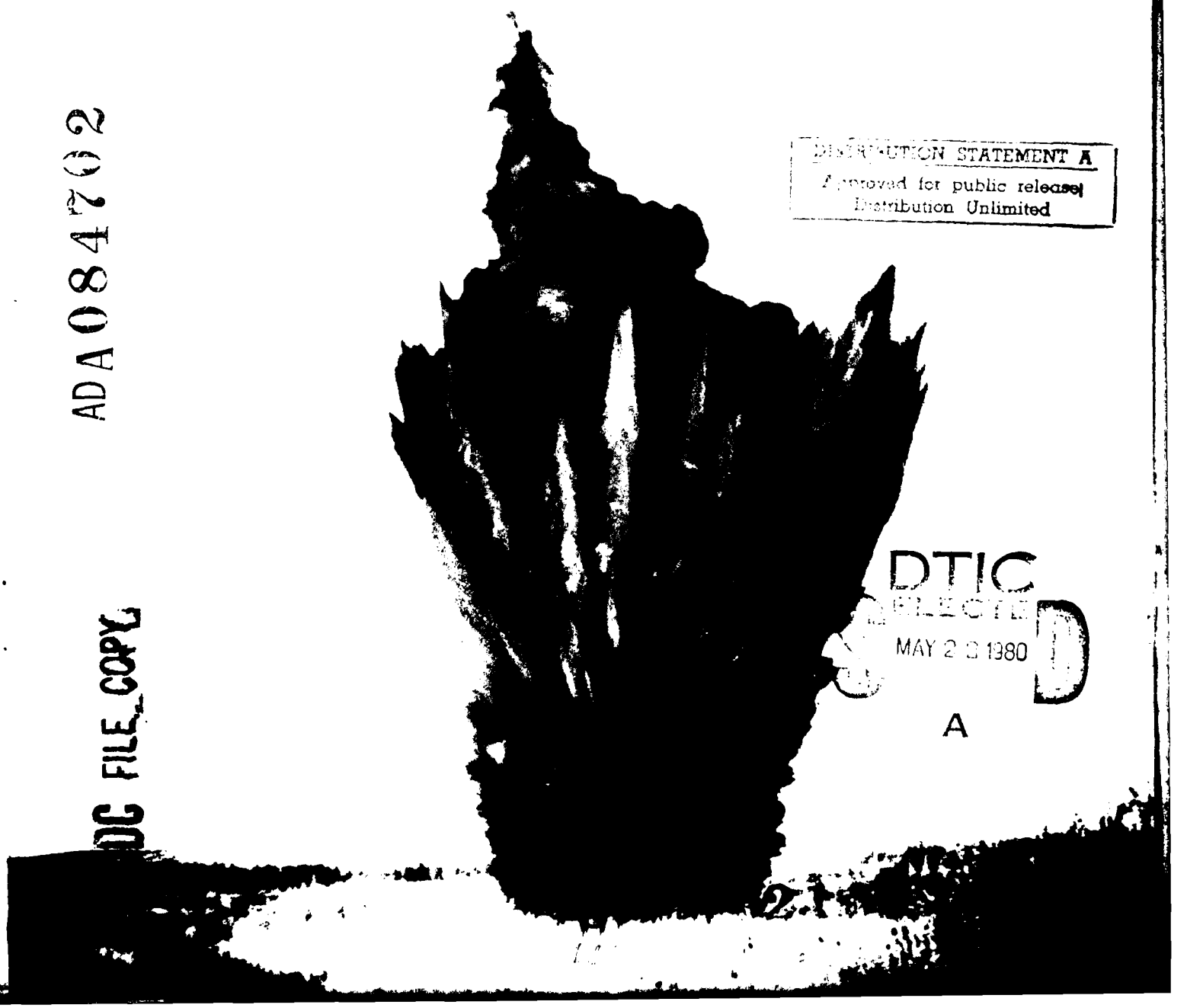

Cover: Large cratering charge of pelletized TNT in thawed silt underlain by permafrost. (Photograph by North Smith.)

14

CRREL Report 80-9

6

High-explosive cratering in frozen and unfrozen soils in Alaska

12 129

10
North Smith

16 4A762719AT45

11
February 1980

17 A31

Prepared for
DIRECTORATE OF MILITARY PROGRAMS
OFFICE, CHIEF OF ENGINEERS
By
UNITED STATES ARMY
CORPS OF ENGINEERS
COLD REGIONS RESEARCH AND ENGINEERING LABORATORY
HANOVER, NEW HAMPSHIRE, U.S.A.

037100

Unclassified

SECURITY CLASSIFICATION OF THIS PAGE (When Data Entered)

REPORT DOCUMENTATION PAGE

READ INSTRUCTIONS BEFORE COMPLETING FORM

1. REPORT NUMBER: CRREL Report 80-9	2. GOVT ACCESSION NO.: AD-A084702
3. RECIPIENT'S CATALOG NUMBER	
4. TITLE (and Subtitle): HIGH-EXPLOSIVE CRATERING IN FROZEN AND UNFROZEN SOILS IN ALASKA	5. TYPE OF REPORT & PERIOD COVERED
	6. PERFORMING ORG. REPORT NUMBER
7. AUTHOR(s): North Smith	8. CONTRACT OR GRANT NUMBER(s)
9. PERFORMING ORGANIZATION NAME AND ADDRESS: U.S. Army Cold Regions Research and Engineering Laboratory, Hanover, New Hampshire 03755	10. PROGRAM ELEMENT, PROJECT, TASK AREA & WORK UNIT NUMBERS: DA Project 4A762730AT42, Task A3, Work Unit 003
11. CONTROLLING OFFICE NAME AND ADDRESS: Directorate of Military Programs, Office, Chief of Engineers, Washington, DC 20314	12. REPORT DATE: February 1980
	13. NUMBER OF PAGES: 26
14. MONITORING AGENCY NAME & ADDRESS (if different from Controlling Office)	15. SECURITY CLASS. (of this report): Unclassified
	15a. DECLASSIFICATION/DOWNGRADING SCHEDULE

16. DISTRIBUTION STATEMENT (of this Report)

Approved for public release; distribution unlimited.

17. DISTRIBUTION STATEMENT (of the abstract entered in Block 20, if different from Report)

18. SUPPLEMENTARY NOTES

19. KEY WORDS (Continue on reverse side if necessary and identify by block number)

Craters
High explosives
Permafrost
Soils

20. ABSTRACT (Continue on reverse side if necessary and identify by block number)

Explosive cratering tests were conducted in seasonally frozen and thawed gravel at Ft. Richardson near Anchorage, Alaska, and in seasonally frozen and thawed silt overlying permafrost and in silt permafrost at Ft. Wainwright near Fairbanks, Alaska. Explosive charge weights ranged from 26 to 3120 lb and charge burial depths ranged from about 3 to 40 ft. The cube root of the charge weight scaling was used to determine maximum scaled crater dimensions and optimum scaled depth of burial of the charge. Test results for frozen and thawed gravel were essentially the same because of the low moisture content and the relatively shallow depth of freezing (5 to 6 ft). The optimum depth of burial of the charge for maximizing the apparent radius and depth and the true radius was about 1.8 times the cube root of the charge weight for both the frozen and thawed conditions. In seasonally frozen silt overlying a talik and

DD FORM 1 JAN 73 1473 EDITION OF 1 NOV 65 IS OBSOLETE

Unclassified

SECURITY CLASSIFICATION OF THIS PAGE (When Data Entered)

20. Abstract (cont'd)

silt permafrost the maximum scaled crater dimensions and optimum scaled burial depths of the charge were smaller than for the thawed condition except for the true crater dimensions. The channeling of energy in the talik produces maximum crater dimensions and an optimum burial depth for the true crater that is larger than for the thawed condition. The results for the homogeneous silt permafrost were very similar to the frozen gravel results with much smaller maximum crater dimensions and smaller optimum charge burial depths than for the thawed silt overlying permafrost. The required charge weight to produce a crater with a given apparent depth is nearly three times greater for silt permafrost than for thawed silt and nearly two times greater for a given apparent crater radius. Mobility tests were conducted with an armored personnel carrier (M-113) in the craters in thawed silt. Two types of craters were effective barriers to normal vehicle travel. One type had a larger diameter than the other and had a fallback mound because of a deeper burial depth. The other had a smaller diameter but had very steep side slopes with the crater blown clear of ejecta.

PREFACE

This report was prepared by North Smith, Research Civil Engineer, of the Geotechnical Research Branch, Experimental Engineering Division, U.S. Army Cold Regions Research and Engineering Laboratory. The research was supported by DA Project 4A762730AT42, *Design, Construction and Operations Technology for Cold Regions,* Task A3, *Cold Regions Military Operations,* Work Unit 003, *Shock Loading in Frozen Earth Media.*

The author appreciates the assistance in field testing received from Arthur S. Gidney and others of the CRREL Alaskan Projects Office and military personnel of the U.S. Air Force at Eielson AFB and of the U.S. Army at Ft. Richardson and Ft. Wainwright. The report was technically reviewed by Dr. M. Mellor, P.V. Sellmann and W.F. Quinn of CRREL.

CONTENTS

ILLUSTRATIONS

TABLES

CONVERSION FACTORS: U.S. CUSTOMARY TO METRIC (SI) UNITS OF MEASUREMENT

These conversion factors include all the significant digits given in the conversion tables in the ASTM *Metric Practice Guide* (E 380), which has been approved for use by the Department of Defense. Converted values should be rounded to have the same precision as the original (see E 380).

Multiply	*By*	*To obtain*
inch	25.4*	millimeter
foot	0.3048*	meter
mile	1.609347	kilometer
pound	0.4535924	kilogram
pound/foot^3	16.01846	kilogram/meter^3
ton	907.1847	kilogram

*Exact

HIGH-EXPLOSIVE CRATERING IN FROZEN AND UNFROZEN SOILS IN ALASKA

North Smith

INTRODUCTION

A problem facing all excavation contractors and military engineering and construction units on their initial encounter with cold regions is the effect of frozen soil moisture on explosive cratering and breakup. Livingston (1959) reported that surface layers of frozen soil could be most effectively broken up by placing the explosive charges of suitable size immediately below the frozen surface layer. More recently, however, Mellor and Sellmann (1974) reported that small charges set in unfrozen material beneath a frozen layer could be quite ineffective in certain types of soil, and they attributed this effect to differences in the compressibility of the unfrozen material. In the saturated soils the compressibility is quite low and the explosives are very effective when placed below the frozen layer, much the same as with submersion of explosives in water below an ice sheet. However, in soils of low moisture and high porosity, high attenuation of the explosive shock is likely to result in merely a camouflet rather than a broken or cratered surface layer.

Larger explosive charges, in the range of 1 to 10 tons (weights applicable to excavation and cratering operations) would seem not to be affected by the thin layers of frozen soil expected in most areas having seasonal frost. Some effect is expected on the fly rock size and on the propagation velocity of elastic Rayleigh waves, but the true and apparent crater dimensions would probably be unaffected. However, in areas of deep seasonal frost (up to 9 ft) and permafrost, significant differences from the unfrozen results seemed probable, and therefore some additional testing was undertaken by CRREL (Smith 1975, 1976a, 1976b, 1976c, 1977) and WES (USAE Waterways Experiment Station) during 1975-76.

Test sites

Three test sites were used for the high explosive cratering tests. One site (Fig. 1), an explosive ordnance demolition (EOD) range, was located at Ft. Richardson, near Anchorage, Alaska. The range had been stripped of organic surface soil leaving a very compact sandy gravel (Fig. 2) with some large cobbles and boulders having a maximum size of 8 in. down to a depth of 3 ft. Below that depth the maximum size increased to 24 in. (Fig. 3). At the time of the frozen condition testing, the gravel was frozen to a depth between 5 and 6 ft. Composite soil moisture profiles for several auger holes are shown in Figure 4. Below the 1-ft depth the moisture contents were generally between 2 and 5%. Snowmelt infiltration near the surface resulted in a thin surface layer with a moisture content ranging between 8 and 25% The snow cover on the test area was removed for the winter tests several days before testing (Fig. 5). The winter tests were conducted in March 1975 and thawed condition tests were conducted in September 1975.

Two test sites consisting of Fairbanks silt (Fig. 6) were located at Fort Wainwright, near Fairbanks, Alaska (Fig. 7) one in a seasonal frost area and one in permafrost. The seasonal frost area had been cleared and stripped of vegetation for military field exercises about 10 years prior to

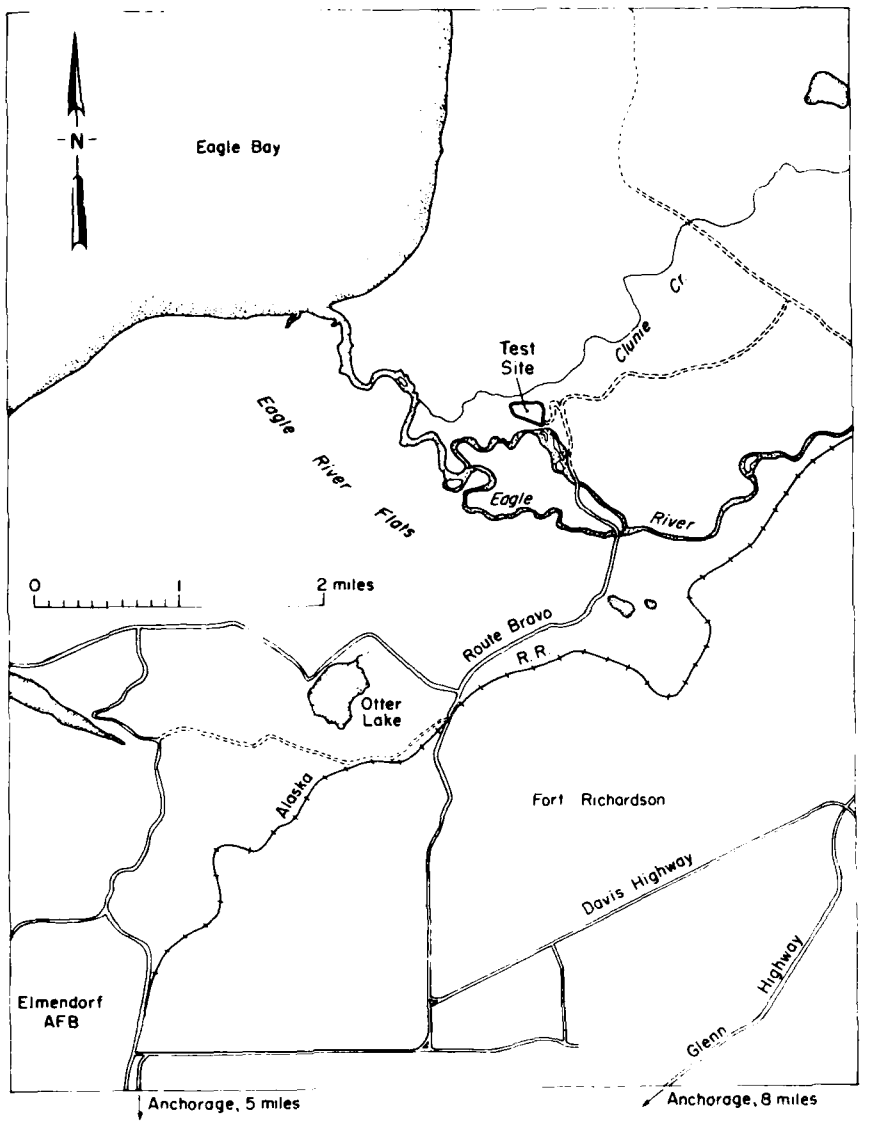

Figure 1. Location of test site (EOD range) at Ft. Richardson.

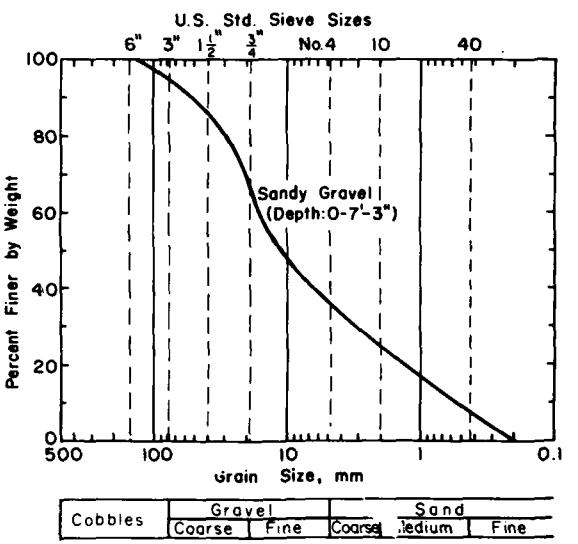

Figure 2. Gravel gradation, EOD range, Fort Richardson.

DEPARTMENT OF THE ARMY
NORTH PACIFIC DIVISION
U.S. ARMY ENGINEER DISTRICT, ALASKA
EXPLORATION LOG

PROJECT: EXPLOSIVE CRATERING, FT. RICH. EAGLE RIVER FLATS — SHEET 1 OF 1
LOCATION (Coordinates or Station): N. E.
DRILLING AGENCY: [X] CORPS OF ENGINEERS [ ] OTHER
HOLE NO. FIELD: AP- 13 PERMANENT: AP- 2663
NAME OF DRILLER: K. MITCHELL
WEATHER:
TYPE OF HOLE: TEST PIT [ ] AUGER HOLE [X] CHURN DRILL [ ]
DEPTH TO:
DEPTH DRILLED INTO:
TOTAL DEPTH OF HOLE: 14.0 ft.
SIZE AND TYPE OF BIT: Williams
DATUM FOR ELEVATION SHOWN: [ ] TBM [ ] MSL
TYPE OF EQUIPMENT: Williams Hole Digger Model PD3s
TOTAL NO OF SAMPLES:
TYPE OF SAMPLES:
DEPTH TO GROUND-WATER:
DATE HOLE STARTED: 24 and 25 March 75 COMPLETED:
EL. TOP OF HOLE: 20 ft.
Geologist: D. FREDRICKSON
Chief, Geology Section:
Chief, Foundations & Materials Branch: Date:

DEPTH FEET	% WATER CONTENT	SAMPLE NO	SOIL LEGEND	CLASSIFICATION	MAX SIZE PARTICLE	FORMATION DESCRIPTION & REMARKS
			GM	Silty Sandy Gravel		Brown, Frozen
			GM/ GP	Silty Sandy Gravel		Brown and Tan, Frozen
2						
4			GP	Sandy Gravel		Brown to Grey, Frozen
6						
	2.4	1	GP	Sandy Gravel	8"	1 Damp, Thawed
8	2.9	2				
	2.6	3	GP	Sandy Gravel	24"	Damp
10						
			GP/ GM	Silty Sandy Gravel		Moist
12	2.8	4				
14	2.7	5				

NPA FORM DEC 1959 19 (REV)

FORT RICHARDSON EAGLE RIVER FLATS

Figure 3. Typical borehole soil log, Fort Richardson EOD range.

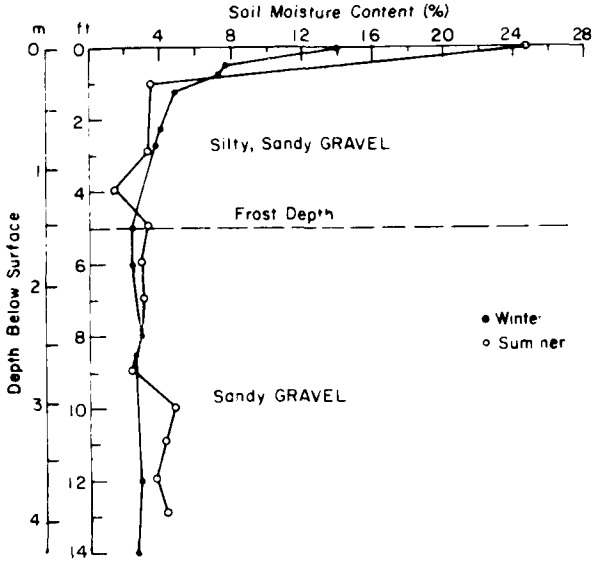

Figure 4. Moisture profiles at Fort Richardson EOD range.

Figure 5. Snow removal at Fort Richardson EOD range.

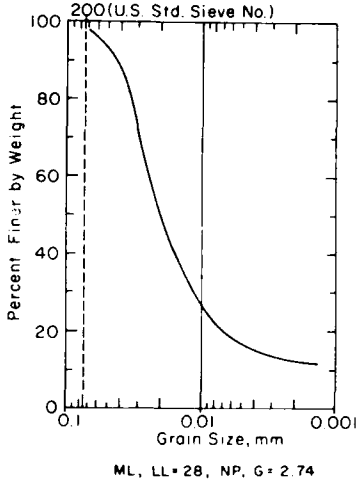

Figure 6. Typical gradation curve for Fairbanks silt.

Figure 7. Location of test sites at Fort Wainwright.

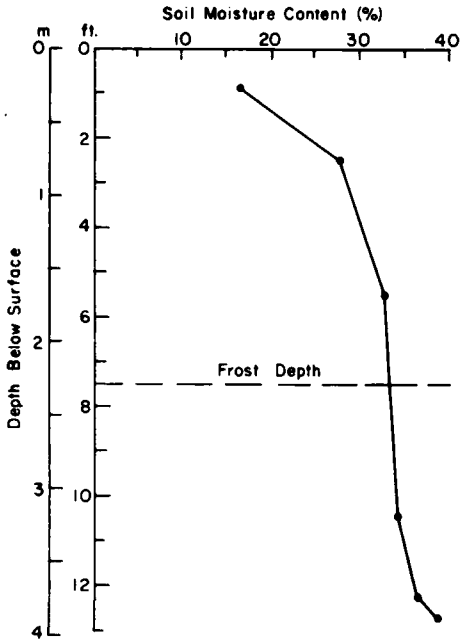

Figure 8. Moisture profile in seasonally frozen silt, Fort Wainwright.

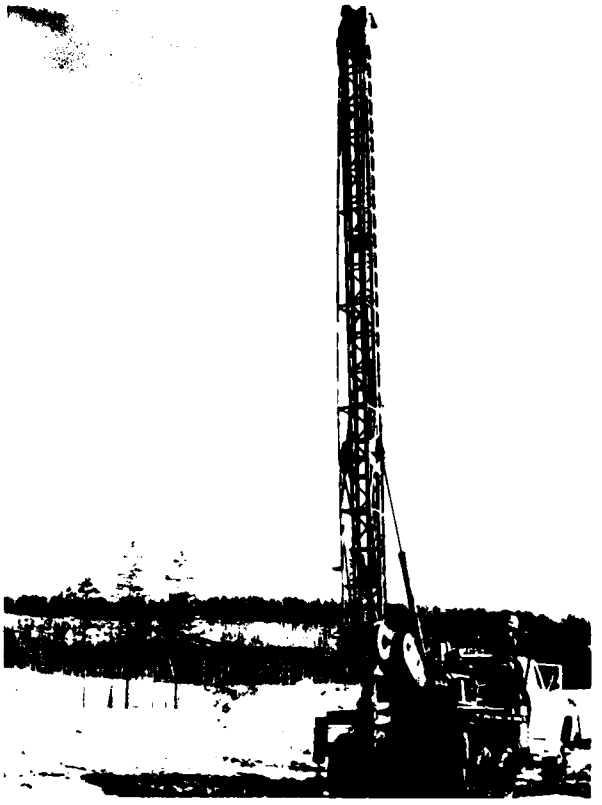

Figure 9. Truck-mounted Williams auger.

these tests, resulting in a surface thaw zone with a maximum thickness of 17 ft overlying silt permafrost during the thawed condition testing in September 1976. During testing in March 1976, the frost zone had an average thickness of 7 ft with a thaw zone (talik) between 7 and 10 ft thick beneath it and overlying the silt permafrost. Moisture conditions for the area are shown in the soil moisture profile of Figure 8. The tests in the permafrost area were conducted in March 1976 in cooperation with the WES testing of a slurry explosive.

Test procedures and materials

All shotholes were augered with truck-mounted Williams augers (Fig. 9). Various bit sizes were tried, with diameters ranging from 12 to 20 in., although most holes had diameters of 18 or 20 in. Auger penetration rates were 10 to 15 ft/hr in the gravel (frozen and unfrozen) and about 8 ft/hr in the frozen silt. [Penetration rates in frozen soils can vary from as low as 2 ft/hr to a high of 120 ft/hr (Sellmann and Mellor 1978).] In the thawed silt, a 14-ft deep hole could be augered in 5 minutes or less (175-200 ft/hr). Augering in the thawed gravel was very troublesome because of the progressive collapse of the hole wall. The wall collapse and the large cobble size at greater depth resulted in a maximum attainable hole depth of between 13 and 14 ft.

Two types of bulk explosive were used in the gravel and seasonal frost test areas, Dupont 60% Pelletol and Canadian Industries Limited (CIL) Nitropel. The two bulk explosives have very similar characteristics; they both are waterproof, pelletized TNT, with a free-pour bulk density of 68 lb/ft^3 and non-cap-sensitivity. The charges were primed with 1-lb primers (approx. one for each 50 lb of explosive) at the ⅓ and ⅔ depths with 150 lb or more of explosives. Detonating cord was used as downlines to the primers and firing of the detonating cord was with no. 6 electric caps on the surface. The shotholes were completely stemmed with auger cuttings after loading and prior to attaching the cap to the detonating cord. Charge weights in the gravel

ranged from 51 to 303 lb, were 300 lb in the seasonally frozen and thawed silt and ranged from 60 to 3120 lb in the silt permafrost.

After each firing, the depth and diameter of the apparent crater were measured, the average lip height was estimated and the surface diameter of the true crater was measured. A schematic drawing (Fig. 10) shows the locations for the crater measurements. Test results and normalized cube-root scaled values are summarized in Tables 1–5.

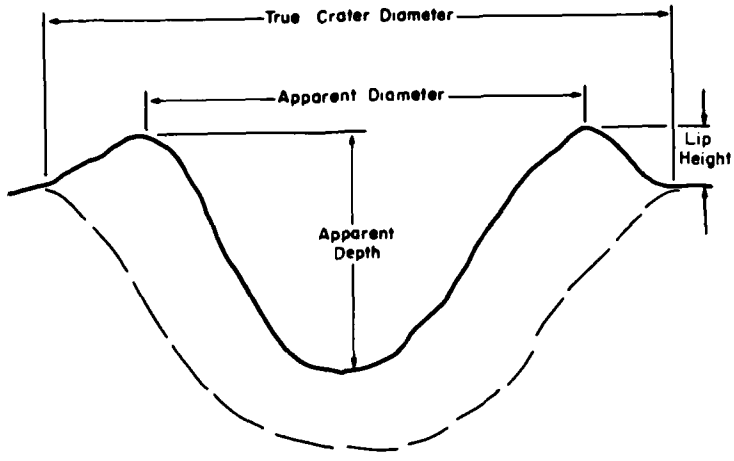

Figure 10. Crater schematic diagram.

Table 1. Results of cratering tests in gravel frozen to a depth of 5 ft.

Charge wt. W (lb)	Sealed charge wt. $W^{1/3}$ ($lb^{1/3}$)	Charge depth* d (ft)	Scaled charge depth $d/W^{1/3}$ ($ft/lb^{1/3}$)	Radius, true crater R_t (ft)†	Scaled radius, true crater $R_t w^{1/3}$ ($lb/ft^{1/3}$)	Radius, apparent crater, R_A (ft)	Scaled radius, crater $R_A/W^{1/3}$ ($ft/lb^{1/3}$)	Depth, apparent crater H (ft)	Scaled depth, apparent crater $H/W^{1/3}$ ($ft/lb^{1/3}$)	Scaled† thickness of frozen layer $t/W^{1/3}$ ($ft/lb^{1/3}$)	Avg. lip height (ft)
102	4.67	5.00	1.07	10.18	2.18	9.35	2.00	4.60	0.98	1.07	1.0
51	3.71	3.00	0.81	7.40	1.99	5.51	1.48	2.60	0.70	1.35	0.5
152	5.34	8.00	1.50	14.32	2.68	10.99	2.06	3.00	0.56	0.94	1.8
51	3.71	7.40	1.99	10.02	2.70	8.68	2.34	2.20	0.59	1.35	1.4
77	4.25	7.20	1.69	11.90	2.80	10.05	2.36	4.40	1.04	1.18	1.2
26	2.96	6.16	2.08	8.15	2.75	6.17	2.08	1.70	0.57	1.69	0.8
203	5.88	9.00	1.53	15.05	2.56	13.04	2.22	6.00	1.02	0.85	1.6
152	5.34	5.90	1.10	13.07	2.45	10.56	1.98	5.90	1.10	0.94	0.8
51	3.71	5.20	1.40	9.48	2.56	7.20	1.94	4.30	1.16	1.35	1.2
303	6.72	11.88	1.77	17.95	2.67	14.62	2.18	3.20	0.48	0.74	2.2
102	4.67	6.50	1.39	13.67	2.93	10.19	2.18	4.80	1.03	1.07	1.8
303	6.72	10.00	1.49	17.73	2.64	14.75	2.19	6.70	1.00	0.74	1.8
223	6.06	7.00	1.16	15.45	2.55	12.38	2.04	5.20	0.86	0.83	1.3
265	6.42	7.25	1.13	17.18	2.68	13.18	2.05	6.30	0.98	0.78	1.7

* To center of gravity.

† Thickness of frozen layer, t = 5.0 ft

Table 2. Results of cratering tests in thawed gravel.

Charge wt. W (lb)	Scaled charge wt. $W^{1/3}$ ($lb^{1/3}$)	Charge depth, d (ft)	Scaled charge depth $d/W^{1/3}$ ($ft/lb^{1/3}$)	Radius, true crater R_t (ft)	Scaled radius, true crater $R_t/W^{1/3}$ ($ft/lb^{1/3}$)	Radius, apparent crater, R_A (ft)	Scaled radius, apparent crater $R_A/W^{1/3}$ ($ft/lb^{1/3}$)	Depth, apparent crater H (ft)	Scaled depth, apparent crater $H/W^{1/3}$ ($ft/lb^{1/3}$)	Avg lip height (ft)
303	6.72	11.4	1.70	25.0	3.72	18.4	2.74	6.50	0.97	2.5
102	4.67	6.20	1.33	14.5	3.10	12.2	2.61	5.00	1.07	1.0
303	6.72	11.1	1.65	17.8	2.65	15.5	2.31	8.40	1.25	1.8
102	4.67	6.80	1.46	12.7	2.72	10.5	2.25	4.80	1.03	0.5
51	3.71	3.20	0.86	8.8	2.37	7.4	1.99	3.70	1.00	1.0
152	5.34	6.80	1.27	15.3	2.86	12.3	2.30	5.60	1.05	0.8
153	5.35	5.80	1.08	14.0	2.62	11.4	2.13	5.30	0.99	0.8
51	3.71	6.20	1.67	10.5	2.83	9.4	2.53	3.00	0.81	1.2
51	3.71	4.60	1.24	10.5	2.83	8.6	2.32	4.00	1.08	1.5
253	6.32	6.50	1.03	15.8	2.50	13.9	2.20	5.70	0.90	0.8
203	5.88	6.40	1.09	18.6	3.16	13.0	2.21	5.30	0.90	1.5
26	2.96	5.40	1.82	10.0	3.38	7.7	2.60	2.40	0.81	0.8
203	4.25	9.60	1.63	21.2	3.60	14.5	2.46	5.50	0.94	2.0
77	4.25	8.00	1.88	13.6	3.20	10.9	2.56	4.00	0.94	1.0

Table 3. Results of cratering tests in frozen silt underlain with a talik and permafrost (charge weight = W = 300 lb, scaled weight = $W^{1/3}$ = 6.67 $lb^{1/3}$).

Charge depth d, (ft)	Scaled charge depth $d/W^{1/3}$ ($ft/lb^{1/3}$)	Radius, true crater R_t (ft)	Scaled radius, true crater $R_t/W^{1/3}$ ($ft/lb^{1/3}$)	Radius, apparent crater R_A (ft)	Scaled radius, apparent crater $R_A/W^{1/3}$ ($ft/lb^{1/3}$)	Depth, apparent crater H (ft)	Scaled depth, apparent crater $H/W^{1/3}$ ($ft/lb^{1/3}$)	Thickness of frozen layer t (ft)	Scaled thickness of frozen layer $t/W^{1/3}$ ($ft/lb^{1/3}$)	Avg. lip height (ft)
3.16	0.47	13.58	2.03	9.92	1.48	8.0	1.20	7.0	1.05	1.0
20.42	3.05	(44.12)*	(6.59)	-	-	(3.0)	(0.45)	7.0	1.05	-
16.96	2.54	34.17	5.11	16.15	2.41	0.5	0.07	7.5	1.12	6.5
7.41	1.11	16.50	2.47	11.50	1.72	4.3	0.64	7.0	1.05	0.5
4.79	0.72	15.16	2.27	10.25	1.53	5.2	0.78	7.0	1.05	0.8
14.58	2.18	44.34	6.63	15.50	2.32	3.0	0.45	9.0	1.34	3.0
9.66	1.44	32.75	4.90	19.34	2.89	5.8	0.87	7.0	1.05	2.2
12.12	1.81	26.25	3.92	17.81	2.66	3.6	0.54	6.5	0.97	2.5

*Numbers in parentheses are mound dimensions for the no-surface-crater condition

Table 4. Results of cratering tests in thawed silt underlain with permafrost (charge weight = W = 300 lb, scaled weight = $W^{1/3}$ = 6.69 $lb^{1/3}$).

Depth to permafrost (ft)	Charge depth d, (ft)	Scaled charge depth $d/W^{1/3}$ ($ft/lb^{1/3}$)	Radius, true crater R_t (ft)	Scaled radius, true crater $R_t/W^{1/3}$ ($ft/lb^{1/3}$)	Radius, apparent crater, R_A (ft)	Scaled radius, apparent crater $R_A/W^{1/3}$ ($ft/lb^{1/3}$)	Depth, apparent crater H (ft)	Scaled depth, apparent crater $H/W^{1/3}$ ($ft/lb^{1/3}$)	Avg. lip height (ft)
15.0	16.6	2.48	40.0	5.98	20.5	3.06	6.5	0.98	2.6
15.6	27.8	4.16	(24.8)*	(3.70)	—	—	(0)	(0)	—
15.6	5.8	0.87	21.0	3.14	14.2	2.12	9.0	1.34	2.2
14.0	16.2	2.42	41.0	6.13	18.4	2.75	5.7	0.86	2.0
15.0	19.1	2.86	33.0	4.93	20.5	3.06	8.3	1.29	2.3
14.0	26.0	3.89	22.5	3.36	13.5	2.02	4.0	0.59	1.8
16.8	7.8	1.17	22.0	3.29	16.0	2.39	8.8	1.32	2.3
14.0	14.6	2.18	31.0	4.63	20.8	3.11	8.2	1.22	2.8
15.0	20.2	3.02	35.0	5.23	17.0	2.54	7.6	1.14	2.0
14.0	23.6	3.53	25.5	3.81	14.0	2.09	6.6	0.99	2.6
16.8	9.3	1.39	23.5	3.51	16.7	2.50	9.8	1.46	2.1
15.6	13.5	2.02	33.0	4.93	20.0	2.99	6.0	0.89	2.6
14.0	21.9	2.02	24.5	3.66	17.0	2.54	5.8	0.86	2.0
14.0	10.6	1.58	33.0	4.93	21.0	3.14	10.0	1.49	3.8

*Numbers in parentheses are mound dimensions for the no-surface-crater condition.

Table 5. Results of cratering tests in silt permafrost.

Shot no.	Charge wt. W (lb)	Scaled charge wt. $W^{1/3}$ ($lb^{1/3}$)	Charge depth d, (ft)	Scaled charge depth $d/W^{1/3}$ ($ft/lb^{1/3}$)	Radius, true crater R_t (ft)	Scaled radius, true crater $R_t/W^{1/3}$ ($ft/lb^{1/3}$)	Radius, crater crater, R_A (ft)	Scaled radius, apparent crater $R_A/W^{1/3}$ ($ft/lb^{1/3}$)	Depth, apparent crater H (ft)	Scaled depth, apparent crater $H/W^{1/3}$ ($ft/lb^{1/3}$)	Avg. lip height (ft)
1	60	3.91	9.19	2.35	15.50	3.96	10.25	2.62	4.00	1.02	0.8
2	60	3.91	4.96	1.27	11.69	2.99	8.50	2.17	4.10	1.05	1.0
3	60	3.91	9.29	2.38	13.65	3.49	8.33	2.66	3.00	0.77	2.0
4	60	3.91	3.27	0.84	11.97	3.06	7.88	2.01	4.25	1.09	0.8
5	60	3.91	11.25	2.88	13.00	3.32	5.00	1.28	3.00	0.77	2.5
6	60	3.91	13.13	3.36	8.10	2.07	3.60	0.92	1.60	0.91	2.2
7	300	6.69	15.30	2.29	20.69	3.09	17.00	2.54	10.95	1.64	—
8	300	6.69	8.75	1.31	17.56	2.62	13.12	1.96	6.80	1.02	1.5
9	300	6.69	11.50	1.72	20.00	2.99	15.04	2.25	4.95	0.74	—
10	300	6.69	5.50	0.82	17.56	2.62	12.43	1.86	6.20	0.93	—
11	300	6.69	18.05	2.70	23.75	3.55	—	—	(4.25)*	(0.64)	—
12	300	6.69	21.55	3.22	20.74	3.10	4.00	0.60	3.20	0.48	1.0
13	3120	14.61	32.15	2.20	—	—	32.78	2.24	8.40	0.57	—
14	3120	14.61	25.90	1.77	50.40	3.45	35.81	2.45	19.10	1.31	—
15	3120	14.61	15.25	1.04	43.80	3.00	32.36	2.22	15.80	1.08	—
16	3120	14.61	39.80	2.72	45.50	3.11	—	—	(9.90)	(0.68)	—

*Numbers in parentheses are mound dimensions for the no-surface-crater condition.

In the silt permafrost test site, a Dow Chemical Company slurry explosive (MS-80-20AL), packaged in plastic bags with 30 lb per bag, was used. The slurry is a sodium and ammonium nitrate blasting agent with a gell-like consistency having 20% by weight of aluminum in foil and atomized forms. The plastic bags were cut open and the slurry was dropped into the shothole to attain a high bulk density. Priming, arming and stemming were the same as for the pelletized explosives. Test results and their cube root scaled values are tabulated in Table 5.

ANALYSIS OF TEST DATA

Relationships between the scaled depth of burial of the charge and scaled measurements of the apparent radius and depth and the true radius of the craters were developed from the data plotted in Figures 11-15. The curves are approximate rather than analytical fits to the data.

The test results for the frozen and thawed gravel are not greatly different. This could be expected since the moisture content was so low that there was little cementation in the frozen state.

Likewise, the test results for the seasonally frozen and thawed silt overlying silt permafrost are also not greatly different with respect to the apparent and true crater radii. However, the maximum scaled apparent depth of crater for the frozen condition was smaller than that for the thawed condition. This is attributed to the presence of the talik (the thawed layer between the seasonal frost surface layer and the underlying permafrost). As the charge is placed deeper into the frozen surface layer, there is the tendency for energy to be directed more into the talik than toward the surface to create a crater. The presence of the talik also seems to produce a slightly larger true radius by channeling the energy to a greater radial distance beneath the frozen surface layer.

The test results for the homogeneous silt permafrost and the frozen layered silt overlying the talik and silt permafrost are nearly the same with respect to the apparent crater radius. The absence of the talik in the homogeneous silt permafrost seems, however, to result in a slightly greater apparent crater depth and a slightly smaller true crater radius than for the layered condition.

The optimum scaled depth of burial (DOB) of the charge for maximizing the apparent crater *radius* was essentially the same at about 1.8 $W^{1/3}$ for the gravel (both frozen and thawed), for the seasonally frozen silt layered condition and for the silt permafrost.

The optimum scaled DOB of the charge for maximizing the apparent crater *depth* varied from a low of 1.0 $W^{1/3}$ for the seasonally frozen silt with the talik underlying it to a high of 1.8 $W^{1/3}$ for the seasonally thawed silt overlying permafrost. The optimum values for the frozen and thawed gravel, and for the silt permafrost were not greatly different at 1.4 $W^{1/3}$ and 1.2 $W^{1/3}$, respectively.

The optimum scaled DOB of the charge for maximizing the true crater radius ranged from 1.8 $W^{1/3}$ for the frozen and thawed gravel to 2.1 $W^{1/3}$ for the silt permafrost and was 2.5 $W^{1/3}$ and 2.6 $W^{1/3}$ for the seasonally thawed and frozen silt overlying permafrost, respectively.

Some quantitative comparisons of the test results for the frozen and thawed conditions and the different soil types can be made from the approximate equations in Figures 11-15. These relationships show that for gravel with a moisture content between about 2 and 8%, the maximum apparent crater radius in the thawed condition was about 11% larger than in the frozen condition. Likewise, the maximum true crater radius in the thawed condition was about 20% larger than in the frozen condition. However, the maximum apparent crater depths and optimum DOB of the charges for both conditions were the same. Much greater variations for the two conditions would be expected if the soil moisture content and the depth of frost were greater.

In the silt seasonal frost area, the maximum apparent crater radius for the thawed condition was about 7% larger and the maximum true crater radius was about 5% smaller than for the frozen condition. These percentages could be considered to be about within the accuracy ($\pm 5\%$) of field measurements. However, the maximum apparent crater depth and the optimum DOB of the charge for the frozen condition were about 33 and 44% smaller, respectively, than for the thawed conditon, indicating the presence of the talik.

In the homogeneous silt permafrost area, the maximum radius and the depth of the apparent crater and the maximum radius of the true crater

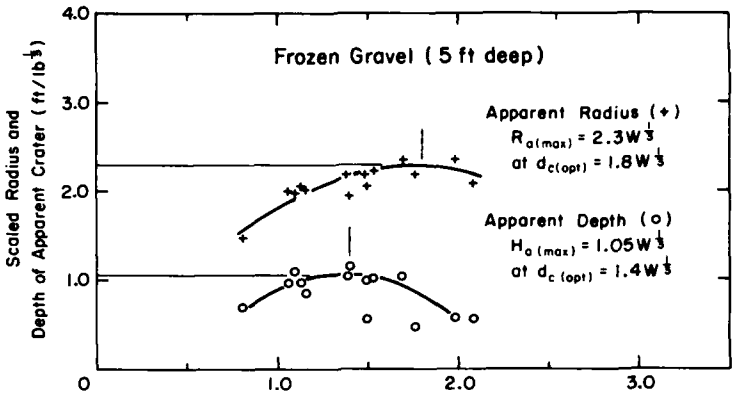

a. Scaled radius and depth of apparent crater for frozen gravel.

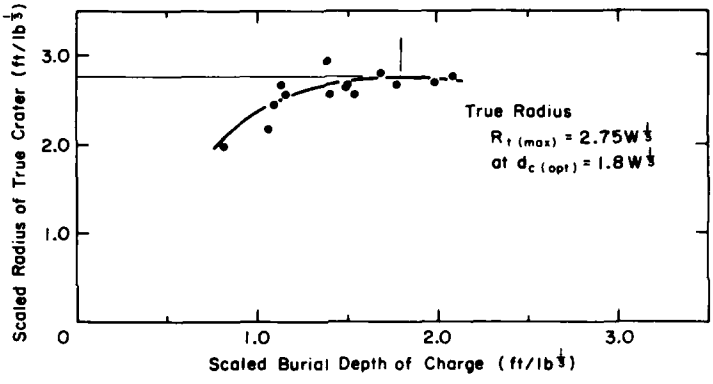

b. Scaled radius of true crater.

Figure 11. Scaled crater dimensions vs scaled burial depth of charge.

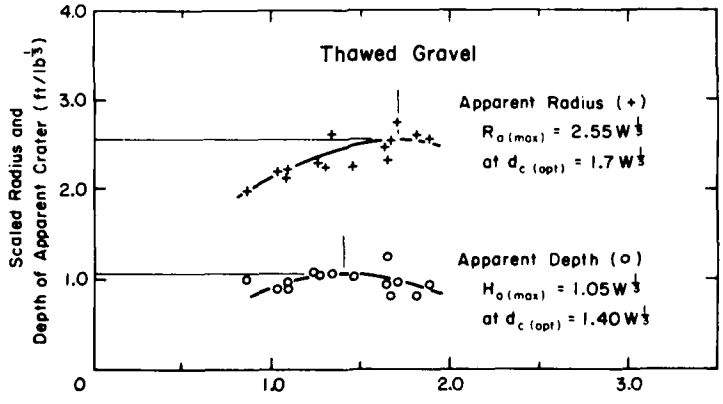

a. Scaled radius and depth of apparent crater.

Figure 12. Scaled crater dimensions vs scaled burial depth of charge for thawed gravel.

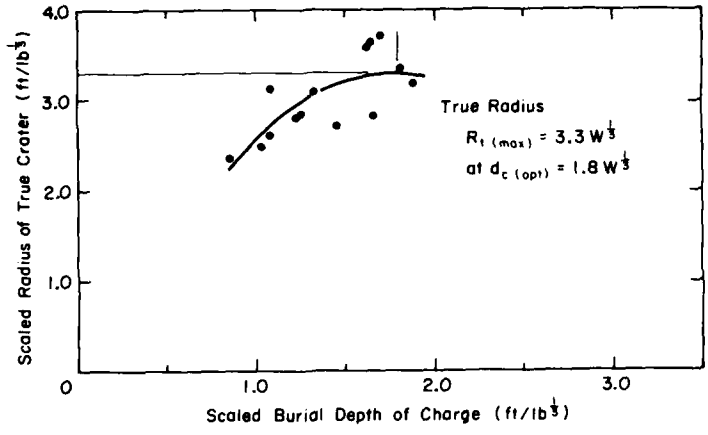

b. Scaled radius of true crater.

Figure 12. (cont'd.) Scaled crater dimensions vs scaled burial depth of charge for thawed gravel.

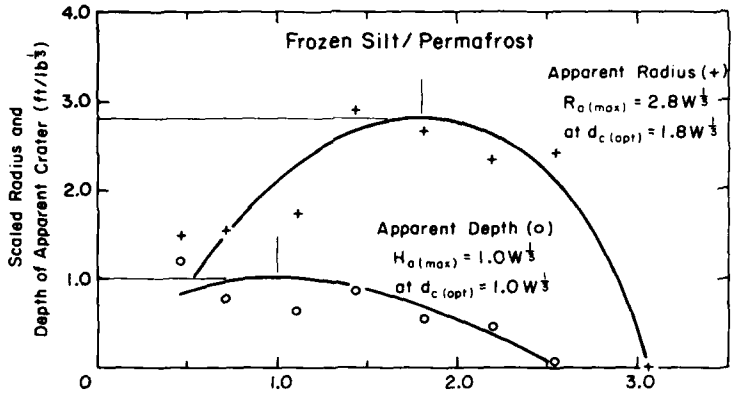

a. Scaled radius and depth of apparent crater.

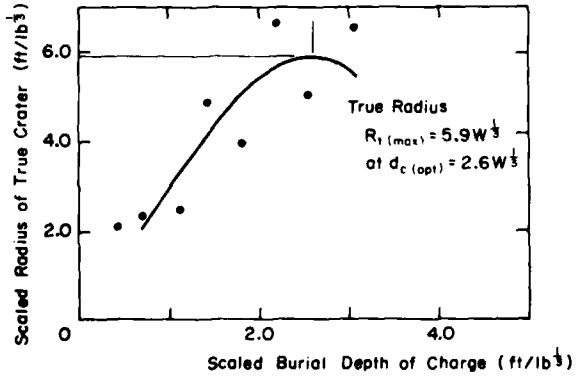

b. Scaled radius of true crater.

Figure 13. Scaled crater dimensions vs scaled burial depth of charge for seasonally frozen silt.

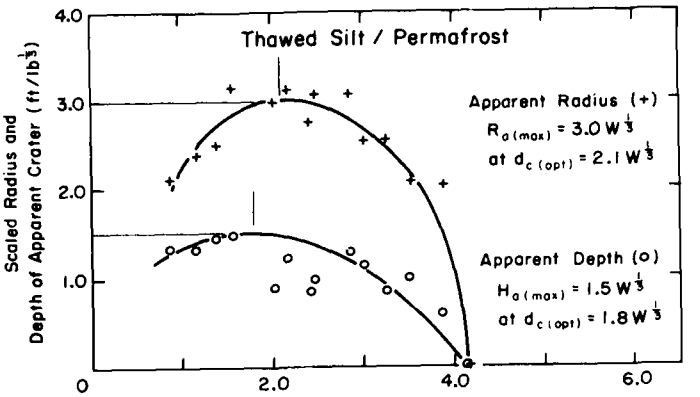

a. Scaled radius and depth of apparent crater.

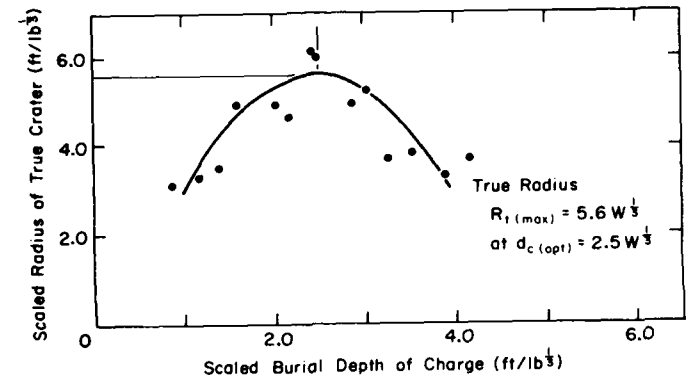

b. Scaled radius of true crater.

Figure 14. Scaled crater dimensions vs scaled burial depth of charge for thawed silt.

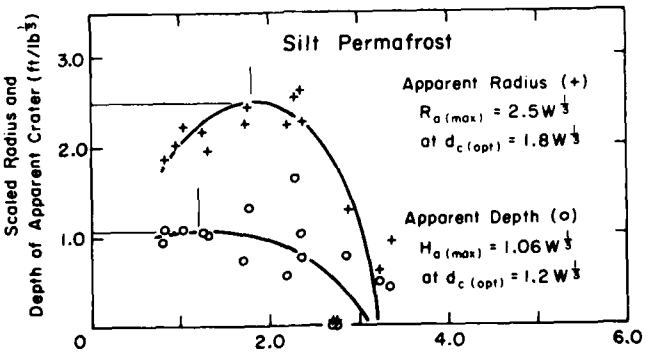

a. Scaled radius and depth of apparent crater.

Figure 15. Scaled crater dimensions vs scaled burial depth of charge for silt permafrost.

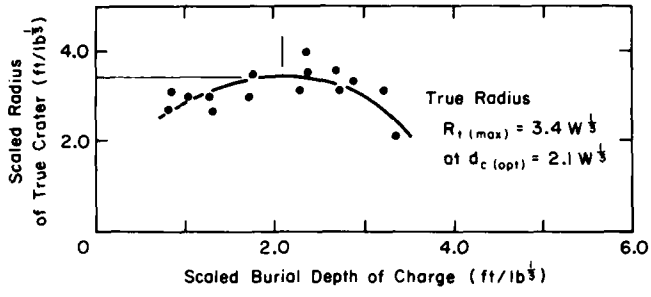

b. Scaled radius of true crater.

Figure 15. (cont'd.) Scaled crater dimensions vs scaled burial depth of charge for silt permafrost.

were smaller than in the seasonally thawed silt by about 17, 29 and 39%, respectively. There is closer agreement between the results for the homogeneous silt permafrost and the seasonally frozen silt with respect to the maximum apparent crater radius and depth but about the same difference for the maximum true crater radius. In the homogeneous silt permafrost the maximum apparent crater radius was 11% smaller, the maximum apparent crater depth was 6% larger and the maximum true crater was 42% smaller than for the seasonally frozen silt.

Generally, in-situ moisture contents of gravels and silts are greatly different, just as was encountered at these test sites. Therefore, a comparison of the results for the two soil types could be very helpful in site selection considerations for certain engineering and tactical applications.

The seasonally frozen silt had maximum apparent and true crater radii about 21% and 114% larger, respectively, than those in the frozen gravel. The maximum apparent depth in the frozen gravel, however, was essentially the same at only 5% larger than that in the seasonally frozen silt. The large difference in the maximum true crater radii is probably not due to the different soil types but to the presence of the talik beneath the seasonally frozen silt surface layer. Also, the higher moisture content and fine grain size of the silt results in crater ejecta of a more cubical form and a surface slab fracturing by bending outward to much greater radial distances than in the drier gravel which fractures mostly by shear.

The thawed silt had a maximum apparent crater depth and maximum apparent and true crater radii that were about 43%, 18% and 70% larger, respectively, than those in the thawed gravel.

There is close agreement in the results for the frozen gravel and the silt permafrost. In the silt permafrost, the maximum apparent crater radius and depth were about 9% and 1% larger, respectively, than those in the frozen gravel. Also, the maximum true crater radius in the silt permafrost was 24% larger than that in the frozen gravel, again indicating the slab fracturing effect.

MOBILITY TESTS

One obvious military application for explosives is the creation of barriers to prevent or slow down troop and equipment movement on the battlefield and supply routes. In conjunction with the crater testing in the seasonally thawed silt overlying silt permafrost, several mobility test runs were made with an armored personnel carrier (APC) M-113 through craters that appeared to present a mobility obstacle. It was discovered that two types of craters presented impassable obstacles for the APC without the assistance of some type of engineering effort (bulldozer work or bridging). These two crater types can be briefly described as follows.

1. A charge buried at a depth in feet of about two times the cube root of the weight ($2.0\ W^{1/3}$) in pounds will produce a crater with a maximum depth in feet of $1.5\ W^{1/3}$. There is generally a fallback mound of ejecta in the center of the crater with a height in feet between $0.3\ W^{1/3}$ and $0.5\ W^{1/3}$ above the bottom of the crater. The radius of the crater in feet is about $3.0\ W^{1/3}$. An APC will nose into the mound upon entering the crater and probably will have to be pulled out

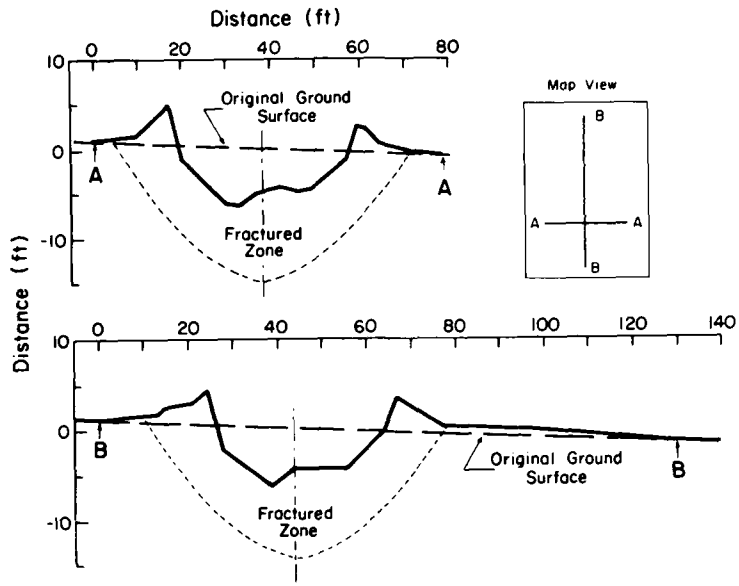

Figure 16. Profiles on perpendicular radii of mobility barrier crater with fallback mound in thawed silt.

Figure 17. Mobility test runs in barrier crater of Figure 16.

(see Fig. 16 and 17). Bridging of the crater will require a minimum of 7.0 $W^{1/3}$ linear feet of bridging.

2. A charge buried at a depth in feet of between 0.8 and 1.4 $W^{1/3}$ will produce a crater with a maximum depth (in feet) of between 1.3 $W^{1/3}$ and 1.5 $W^{1/3}$. Generally, the crater is blown clear of ejecta and has quite steep side slopes (see Fig. 18 and 19). The maximum radius of the crater in feet is between 2.1 $W^{1/3}$ and 2.5 $W^{1/3}$. Bridging of the crater would require a minimum of 6.0 $W^{1/3}$ linear feet of bridging.

Both types of craters can be breached rather quickly and easily with the assistance of a bulldozer. However, it would be essentially suicidal not to have multiple breaching points through a barrier system of craters. Therefore, several armored bulldozers would probably be needed in the theater of operations (an added logistics requirement for the advancing enemy force). The second type of crater requires more bulldozer effort because of the absence of the center mound of ejecta and the steepness of the side slopes. The choice of crater type to be used will depend on the bridging capabilities of the enemy forces and the available time to create the barrier system. If a hasty barrier system were required, the second type of crater would probably be used in order to take advantage of the lesser drilling time.

The empirical relationships developed from the data plots in Figures 11-15 are plotted in Figures 20-24 in a form to show how crater dimensions and burial depths of the charge vary with the charge weight. A significant difference (an approx. factor of 3) is seen in the weight of explosive charge required to obtain a crater of equal apparent depth in the thawed and frozen silt. However, the gravel with low moisture content required approximately equal weights of explosive for equal apparent crater depths in the frozen and thawed conditions.

WES conducted mobility tests with an APC through the craters in the homogeneous silt permafrost. Complete data for these tests are not available, but the nature of the breakup of the frozen silt makes for poorer traction and a lower speed than for the thawed condition because of

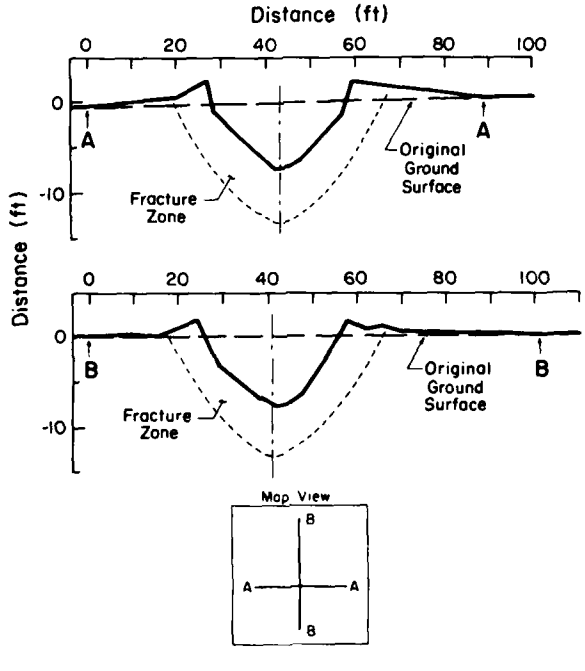

Figure 18. Profiles on perpendicular radii of mobility barrier crater without fallback mound in thawed silt.

Figure 19. Mobility test runs in crater of Figure 18

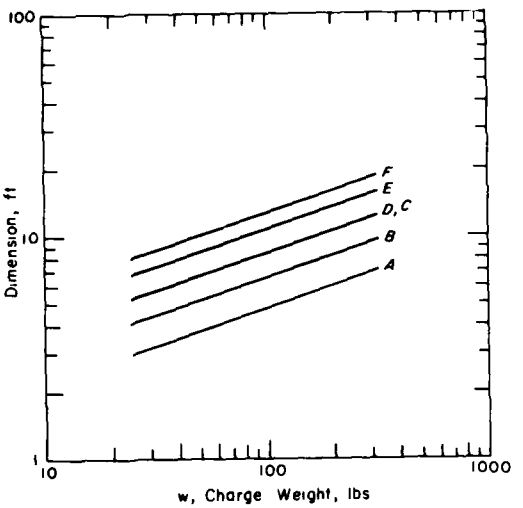

Figure 20. Maximum crater dimensions and optimum burial depth of charge vs charge weight for frozen gravel. (A—maximum apparent crater depth, B—optimum burial depth to maximize apparent crater depth A, C—optimum burial depth of charge to maximize apparent crater radius E, D—optimum burial depth of charge to maximize true crater radius F, E—maximum apparent crater radius, F—maximum true crater radius.)

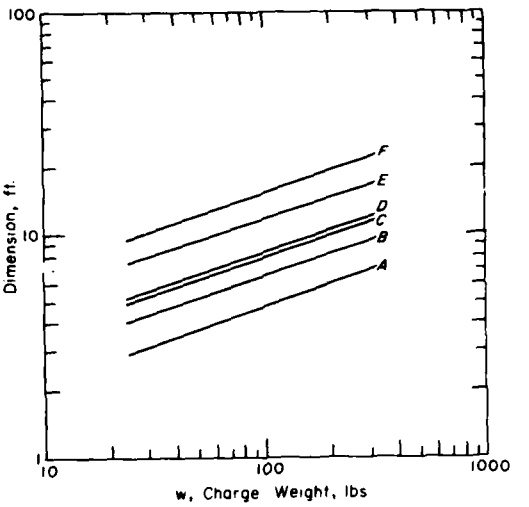

Figure 21. Maximum crater dimensions and optimum burial depth of charge vs charge weight for thawed gravel.

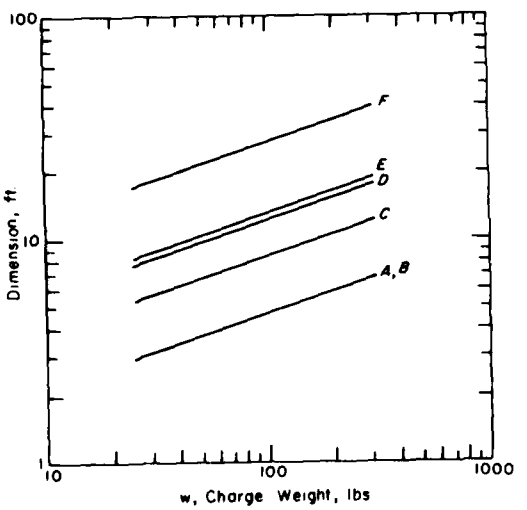

Figure 22. Maximum crater dimensions and optimum burial depth of charge vs charge weight for frozen silt underlain by a talik and silt permafrost.

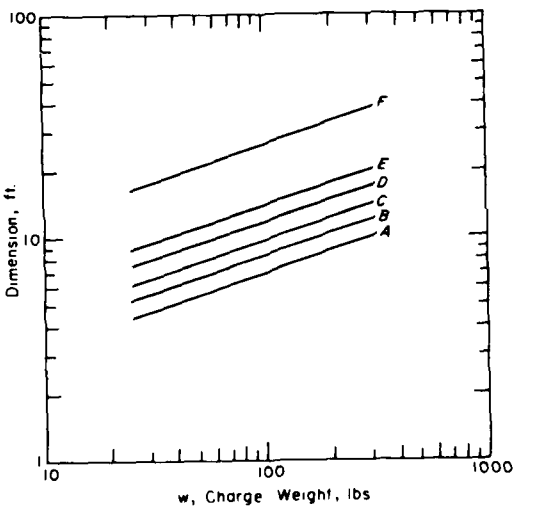

Figure 23. Maximum crater dimensions and optimum burial depth of charge vs charge weight for thawed silt underlain with silt permafrost at depth of 14 to 17 ft.

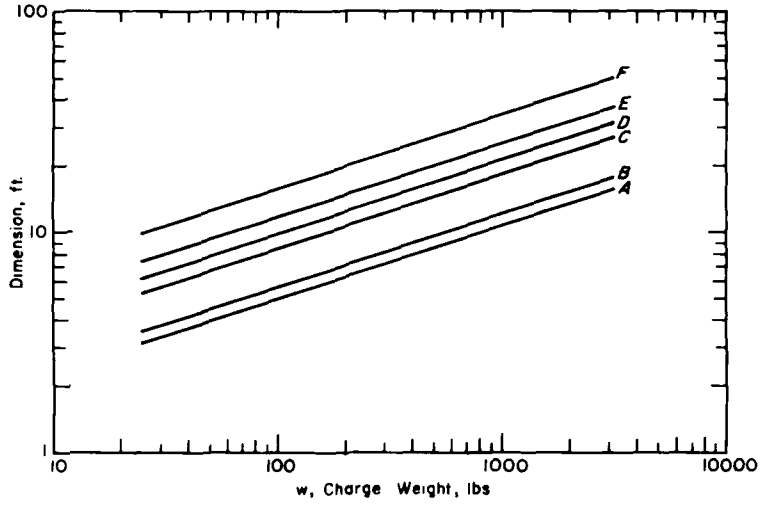

Figure 24. Maximum crater dimensions and optimum burial depth of charge vs charge weight for silt permafrost.

a. Burial depth = 0.7 $W^{1/3}$.

Figure 25. Mobility barrier of fractured frozen silt crater ejecta.

b. Burial depth = 1.44 $W^{1/3}$

Figure 25. (cont'd.) Mobility barrier of fractured frozen silt crater ejecta.

the surface roughness. In fact, the fractured frozen silt strewn on the surface like a boulder field will make vehicular movement much more difficult, slower, and more vulnerable to defensive firepower even if the craters are small. Charge burial depth for such barrier systems can be quite shallow (Fig. 25).

CONCLUSIONS

In gravel with a low moisture content (2 to 8%), the craters for the thawed condition will have radii larger than those for the frozen condition by about 10 and 20% for the apparent and true dimensions, respectively, and will have about equal apparent depths. For both the frozen and thawed conditions, the optimum DOB of the charge will be about 1.8 $W^{1/3}$ for maximizing the apparent and true crater radii and about 1.4 $W^{1/3}$ for maximizing the apparent crater depth.

In silt with an average moisture content of about 30%, the craters for the thawed layer overlying permafrost will have larger apparent and true radii than those in homogeneous silt permafrost by about 20 and 65%, respectively. The optimum DOB of the charge for maximizing the apparent crater radius in the thawed condition is about 17% deeper than in the permafrost. For the true radius, the percentage is only slightly higher at 19%. The apparent crater depth in the thawed conditon is about 42% larger than that in the permafrost, and the optimum DOB of the charge is about 50% deeper for the thawed condition.

The seasonally frozen silt overlying a talik and permafrost will have larger apparent and true crater radii than the permafrost by about 12 and 74%, respectively, because of energy channeling in the talik. The optimum DOB's of the charges for maximizing the apparent and true crater radii in the layered system are equal and 24% larger, respectively, than in the permafrost. The optimum DOB of the charge for maximizing the apparent crater depth is essentially the same at 1.0 $W^{1/3}$ and 1.06 $W^{1/3}$ for the layered and homogeneous conditions, respectively.

Craters in the silt permafrost with 30% soil moisture will have maximum apparent radii and depths less than 10% larger than those in frozen gravel with 2 to 8% soil moisture. However, the true crater radius in the silt permafrost will be about 24% larger than that in the frozen gravel due to the slab fracturing effect in the silt permafrost. The optimum DOB of the charge for

maximizing the apparent crater radius is the same in the two materials at about 1.8 $W^{1/3}$. The optimum DOB of the charge for maximizing the apparent crater depth in the gravel is about 17% deeper than for the silt permafrost, 1.4 $W^{1/3}$ and 1.2 $W^{1/3}$, respectively. The optimum DOB of the charge for maximizing the true crater radius in the silt permafrost is about 17% deeper than for the gravel, 2.1 $W^{1/3}$ and 1.8 $W^{1/3}$, respectively.

Two types of craters in thawed silt are effective barriers against APC movement. For one type, charges buried at depths of about 2.0 $W^{1/3}$ will produce craters with depths of 1.5 $W^{1/3}$ and radii of 3.0 $W^{1/3}$. There will generally be a center mound of ejecta fallback which might make it easier to bridge the craters. However, some engineering effort will be necessary to breach them. For the other type, charges buried at depths of 0.8 to 1.4 time $W^{1/3}$ will produce craters with depths of 1.2 to 1.5 times $W^{1/3}$ and radii of 2.3 times $W^{1/3}$. The craters are blown clear of ejecta and have steep side slopes. Bridging and/or dozer work will be required to breach them.

The weight of explosive required to produce an equal apparent crater radius in silt is greater by a factor of about two for the frozen condition and by a factor of about three to produce a crater with an equal apparent depth.

In frozen silt the cubical form of the ejecta makes for poor traction and surface roughness, which drastically slow vehicular movement and increase vulnerability to defensive firepower.

LITERATURE CITED

Livingston, C.W. (1959) Excavations in frozen ground, Part II Explosion tests in frozen glacial till, Ft. Churchill, 1959. CRREL Technical Report 30, AD 233474.

Mellor, M. and P.V. Sellmann (1974) Blasting tests in seasonally frozen ground. CRREL Technical Note (unpublished)

Smith, N. and M. Mellor (1975) High explosive cratering in seasonally frozen gravel. CRREL Technical Note (unpublished)

Smith, N. (1976a) Cratering of silt permafrost using a slurry explosive. CRREL Technical Note (unpublished)

Smith, N. (1976b) High explosive cratering in seasonally frozen permafrost layered silt formations. CRREL Technical Note (unpublished)

Smith, N. (1976c) High explosive cratering in thawed gravel. CRREL Technical Note (unpublished)

Smith, N. (1977) High explosive cratering in a thawed permafrost layered silt formation. CRREL Technical Note (unpublished)

Sellmann, Paul V. and M. Mellor (1978) Large mobile drilling rigs used along the Alaska pipeline. CRREL Special Report 78-4, AD A053536.

A facsimile catalog card in Library of Congress MARC format is reproduced below.

Smith, North
High-explosive cratering in frozen and unfrozen soils in Alaska/by North Smith. Hanover, N.H.: U.S. Cold Regions Research and Engineering Laboratory; Springfield, Va.; available from National Technical Information Service, 1980.
v, 26 p., illus.; 28 cm. (CRREL Report 80-9.)
Prepared for Directorate of Military Programs, Office, Chief of Engineers, by Corps of Engineers, U.S. Army Cold Regions Research and Engineering Laboratory, under DA Project 4A762730AT42.
Bibliography: p. 20.
1. Craters. 2. High explosives. 3. Permafrost. 4. Soils. I. United States. Army Corps of Engineers. II. Army Cold Regions Research and Engineering Laboratory, Hanover, N.H. III. Series: CRREL Report 80-9.

U.S. GOVERNMENT PRINTING OFFICE: 1980—600-420/429